Analysis and Design of Focused Interdigital Transducers

Tsung-Tsong Wu, He-Tai Tang, Yung-Yu Chen, and Pei-Ling Liu

Abstract—Focused interdigital transducers (FIDTs) can generate surface acoustic wave (SAW) with high intensity and high beamwidth compression ratio. Owing to these features, they are very suitable to be used as the sources of microacoustic channels or waveguides in the near future. The focusing properties of FIDTs are dominated solely by their geometric shapes. Therefore, to obtain optimal performance, it is essential to analyze the FIDTs with a variety of geometric shapes. However, among the existing studies concerning the diffraction of FIDTs, a detailed analysis and design of FIDTs is still in paucity. In this paper, we adopted the exact angular spectrum of plane wave theory (ASoW) to calculate the amplitude fields of FIDTs on Y-Z lithium niobate (LiNbO$_3$) with the shape as a concentric circular arc and the concentric wave surface. Based on the calculation results, we discussed the variations of the amplitude fields induced by changing number of pairs, degree of arc, and geometric focal length. In addition, the focusing properties of FIDTs on the (100)-oriented GaAs substrate were also analyzed and discussed. We also summarized the guiderules for designing a FIDT via four important factors. It is worth noting that the results of this study provide an important basis for designing various FIDTs to fit the desired applications.

I. Introduction

THE focused interdigital transducer (FIDT) has been used widely in many applications recently due to its advantages of achieving high intensity and large beamwidth compression ratio. In signal processing, they were used as convolvers [1]–[4], time-Fourier transformers [5], and radio frequency (RF) channelizers [6]. As to optical communication, acousto-optic tunable filters (AOTF) with FIDTs can improve their performance effectively [7], [8]. In acousto-electric (AE) applications, FIDTs can generate high intensity acoustic field and enhance AE effect to manipulate electron-hole pairs in GaAs quantum well [9]. An experimental study on the surface acoustic wave (SAW) band gap of two-dimensional (2-D) phononic structures in micrometer scale was proposed recently [10]. To realize a phononic crystal waveguide with a line defect (as shown in Fig. 1), a device that can provide SAW sources with high intensity and large beamwidth compression ratio is needed. The FIDT is very suitable for this application.
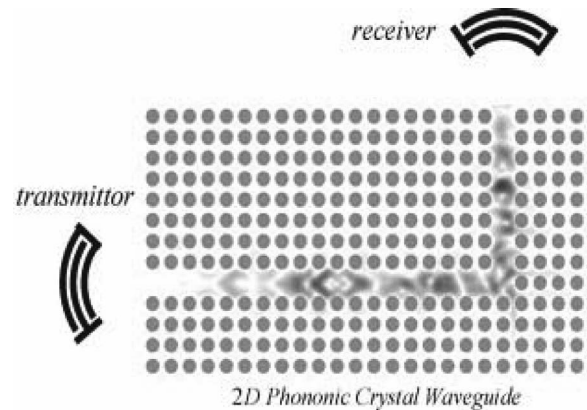
Fig. 1. Schematics of FIDTs and a 2-D phononic crystal waveguide.

The FIDT was first discussed by Kharusi and Farnell [11] in 1972. They proposed two sets of FIDTs with shapes that are a circular arc and wave surface, respectively. The results show that both of them are able to focus SAW and the FIDT with the shape as the wave surface has better focusing properties. In addition, they emphasized that the focusing properties of the FIDTs become worse when increasing number of pairs. Green and Kino [1], and Green *et al.* [2] used Huygen's principle to calculate the amplitude field of a FIDT with circular-arc shape and predicted that the amplitude field has only one focal point. However, according to Fang and Zhang's [12] calculation and experimental results in 1989, this amplitude field has no focal point, but a very long and narrow SAW beam in the main propagation direction. In 2003, de Lima *et al.* [13] studied the amplitude field of a FIDT on the (100)-oriented GaAs substrate. Although FIDT has been proposed over three decades, most of the literature simply involved the simple "curved" interdigital transducers (IDTs) and did not concentrate on the design of FIDTs. In this paper, we present detailed analysis and design of a focused-type SAW transducer by angular spectrum of plane wave theory.

II. Angular Spectrum of Plane Wave Theory

As shown in Fig. 2, we set the X-Y plane on the surface of a piezoelectric material and the IDT's fingers are along the Y-axis. If the cut of the substrate is fixed, the wave vector $\bar{k}$ can be expressed as a function of the propagation angle ϕ. In addition, we assume that there are no dispersion and propagation loss in the half-infinite substrate, so plane harmonic waves on this surface can be expressed
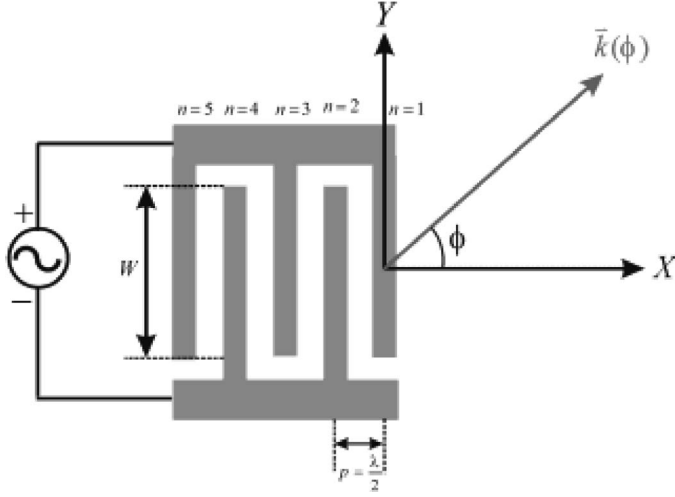
Fig. 2. Illustration of a conventional straight interdigital transducer.

Fig. 3. FIDTs with the shape as (a) the conventional structure and (b) the concentric structure.

as $\exp[-j(Xk_x + Yk_y)]$, where k_x and k_y are the X and Y components of wave vector $k(\phi)$, respectively. Furthermore, because the system is linear, the total amplitude distribution can be evaluated by a scalar field [14] as:

$$\psi_T(X,Y) = \\ \sum_{i=1}^{N} \frac{1}{2\pi} \int_{-\infty}^{\infty} \overline{\psi}_i(k_y) \exp\left[-j\left\{x_i k_x(k_y) + y k_y\right\}\right] dk_y \\ \text{for } X \geq 0, \quad (1)$$

where X'_i is equal to $0, -p, -2p, -3p, \ldots, -Np$ and N is the finger number of IDT. $\overline{\psi}_i(k_y)$ is the inverse Fourier transform of the acoustic source function $\psi_i(X'_i, Y')$ and is expressed as:

$$\overline{\psi}_i(k_y) = \int_{-\infty}^{\infty} \psi_i(X'_i, Y') \exp(jY'k_y) dY'. \quad (2)$$

The acoustic source function $\psi_i(X'_i, Y')$ is taken as:

$$\psi_i(X'_i, Y') = \begin{cases} A \cdot (-1)^{|X'_i/p|} & |Y'| < \dfrac{W}{2} \\ \dfrac{A}{2} \cdot (-1)^{|X'_i/p|} & |Y'| = \dfrac{W}{2} \\ 0 & |Y'| > \dfrac{W}{2} \end{cases}, \quad (3)$$

where W is the aperture of IDT, A is an arbitrary constant, and p is the period of metal strips of IDT. Based on (1), (2), and (3), we can calculate the amplitude field of a conventional straight IDT on the surface of a half-infinite substrate.

III. FIDTs With the Shape as a Concentric Circular Arc

A FIDT with circular-arc shape [as shown in Fig. 3(a)] was used frequently because of its simplicity. However, when its finger number increases, the focusing properties
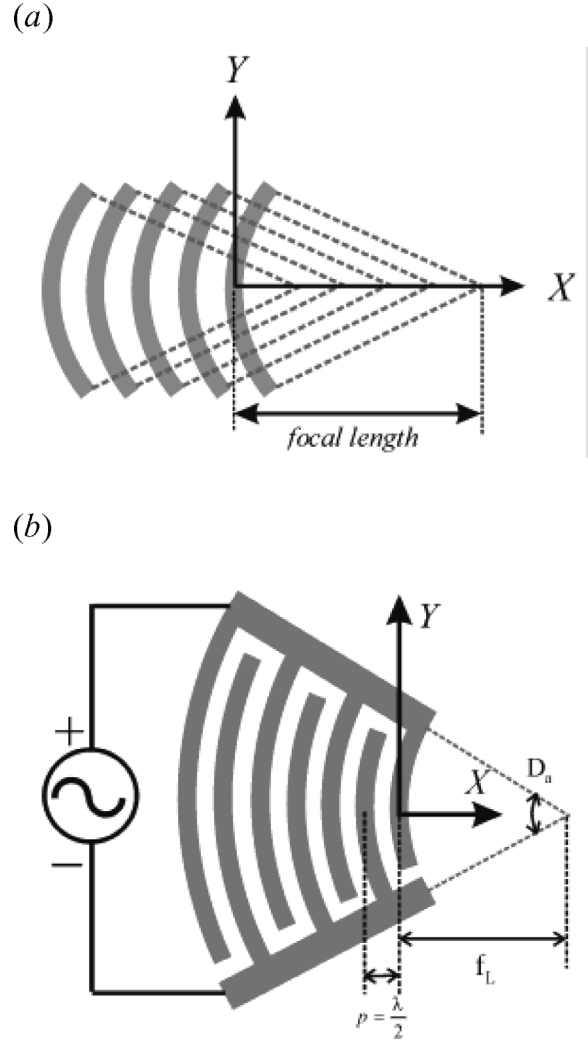
become unstable. In order to overcome this drawback, the concentric structure, as shown in Fig. 3(b), is adopted to be the shape of our FIDT. The amplitude field of a FIDT with the shape as a concentric circular arc can be calculated by using the ASoW theory as long as the acoustic source function is modified by the equivalent aperture method. The equivalent aperture method, presented by Kharusi and Farnell [11], describes that a curved IDT can be approximated by a straight IDT with equiphase distribution. Therefore, the new acoustic source function is given by:

$$\psi'_i(X'_i, Y') = \psi_i(X'_i, Y') \cdot \exp[jk_0 \cdot \Delta(X'_i)], \quad (4)$$

where $\psi_i(X'_i, Y')$ as shown in (3), is the acoustic source function of the straight IDT. $\Delta(X'_i)$ is the path difference between the real aperture and the equivalent aperture of ith finger of the curved IDT. According to (1), (2), and (4), the total amplitude field of a FIDT with the shape as a concentric circular arc can be calculated.

To design a FIDT, three design parameters must be considered: number of pairs N_p, degrees of arc D_a, and
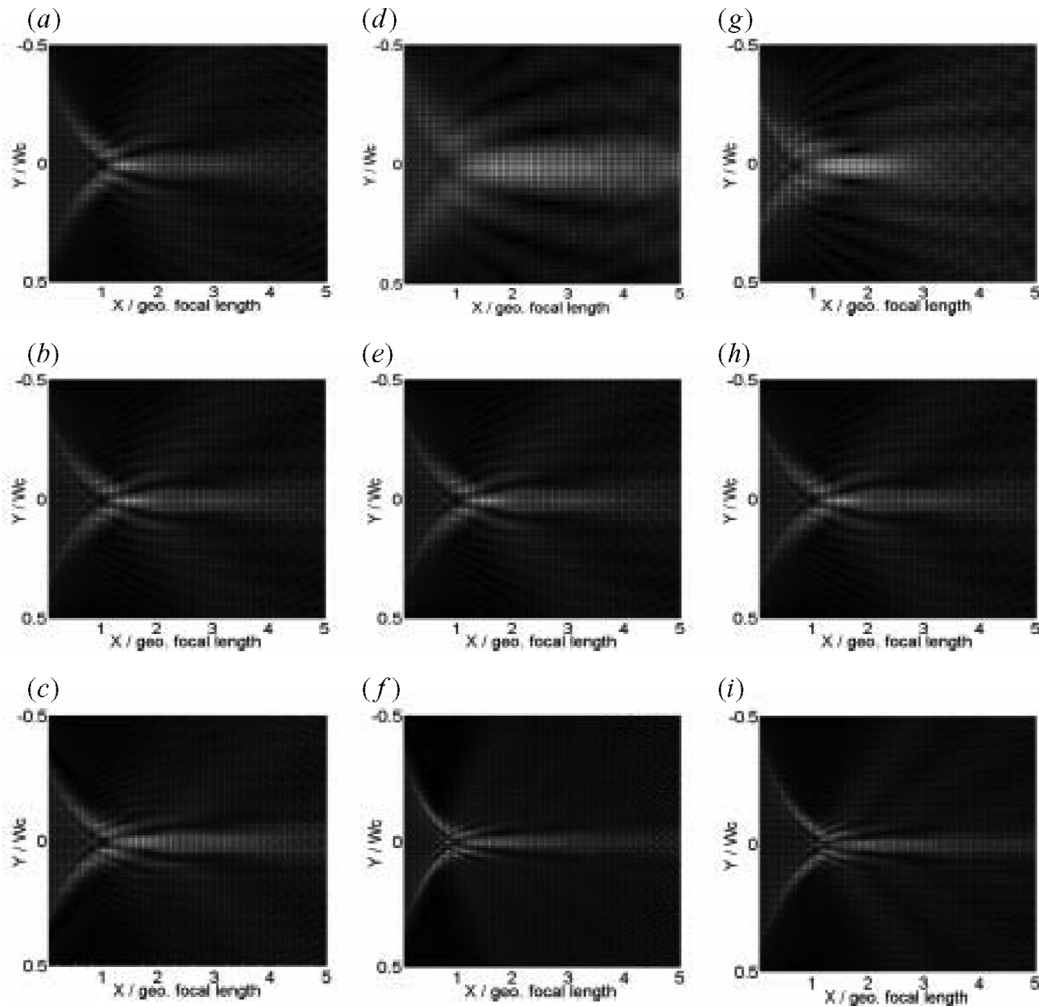
Fig. 4. Total amplitude fields of FIDTs with the shape as a concentric circular arc. (a) Design 1-1, (b) design 1-2, (c) design 1-3, (d) design 2-1, (e) design 2-2, (f) design 2-3, (g) design 3-1, (h) design 3-2, (i) design 3-3.

TABLE I
FIDTs WITH A VARIETY OF DESIGNS.

Design parameters	Number of pairs (N_p)	Degree of arcs $D_a)$	Geo. focal length (f_L)	Wave length (λ)
Design 1-1	5 pairs	40°	50 λ	58.13 μm
Design 1-2	10 pairs	40°	50 λ	58.13 μm
Design 1-3	20 pairs	40°	50 λ	58.13 μm
Design 2-1	10 pairs	20°	50 λ	58.13 μm
Design 2-2	10 pairs	40°	50 λ	58.13 μm
Design 2-3	10 pairs	60°	50 λ	58.13 μm
Design 3-1	10 pairs	40°	25 λ	58.13 μm
Design 3-2	10 pairs	40°	50 λ	58.13 μm
Design 3-3	10 pairs	40°	100 λ	58.13 μm

geometric focal length f_L. Nine sets of different design parameters are listed on Table I, where λ means the wavelength of SAW excited by a FIDT. In general, λ is equal to twice the period of the metal strips. In the following, we discuss one by one how the design parameters affect the amplitude fields. The substrate we used here is Y-Z LiNbO$_3$.

A. Number of Pairs (N_p)

The design parameters are listed in design 1-1 to 1-3 of Table I, and the corresponding simulated results are shown in Figs. 4(a)–(c). In Figs. 4(a)–(c), we observe that, because of the concentric structure, the total amplitude fields are quite similar no matter how many N_p are. Furthermore, the total amplitude fields have a narrow, long, strong SAW beam, not a focal point. The results are consistent with Fang's experimental results [12]. Besides, as shown in Fig. 5(a), the amplitude is proportional to N_p.

The beamwidth compression ratio η_c is defined as:

$$\eta_c = \frac{H}{W_c}, \tag{5}$$

where H is the 3 dB transverse beamwidth and W_c is the equivalent aperture of the central finger of FIDT. Fig. 5(a) also shows that the beamwidth compression ration η_c does not change obviously when we change N_p. In Fig. 5(c), we observe that the amplitude field has a peak at about 1.5 times of the geometric focal length (f_L). It is worth noting that the amplitude maintains half of its maximum amplitude until about 4 times the f_L.
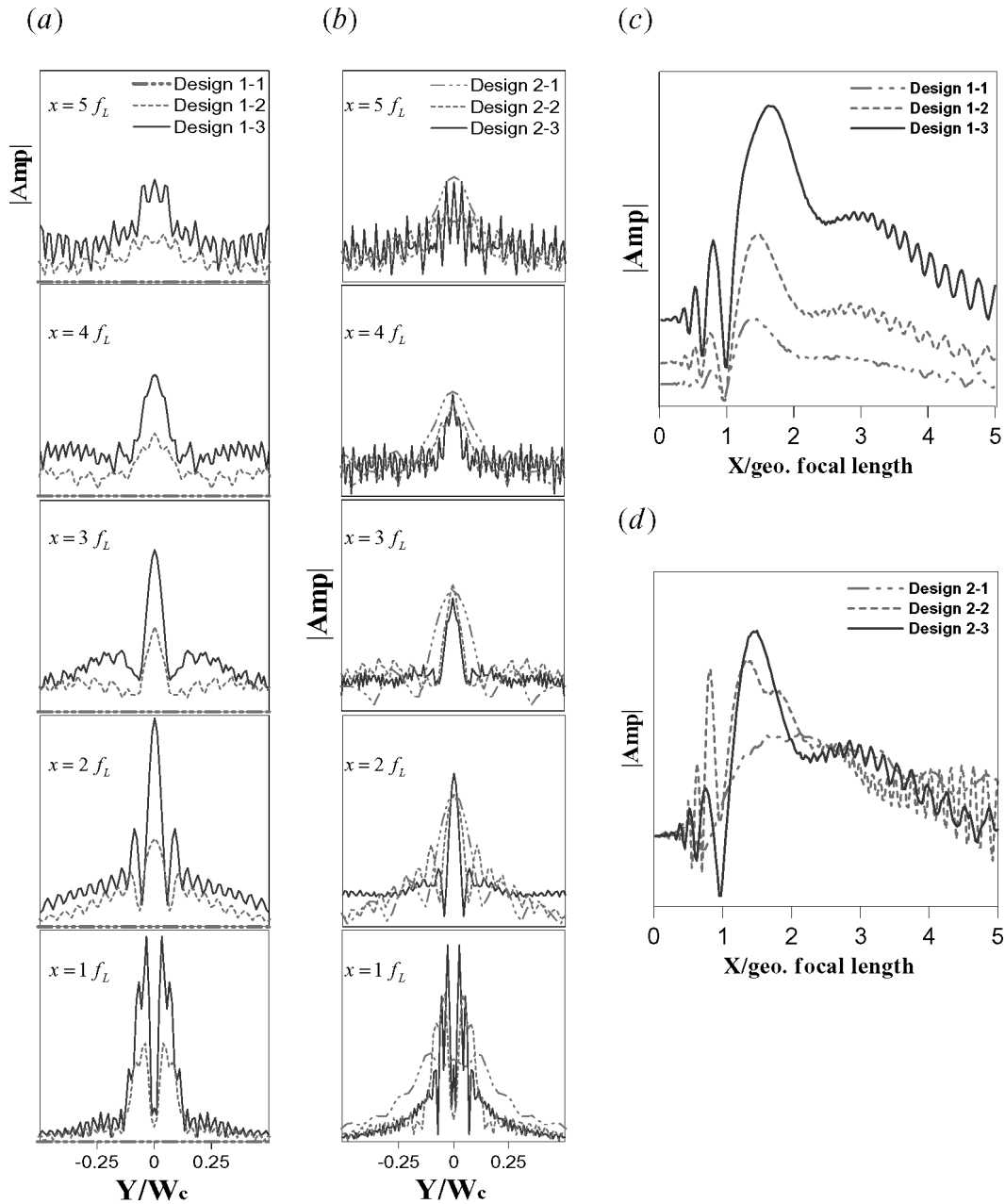
Fig. 5. Cross sections of amplitude fields of FIDTs with the shape as a concentric circular arc. (a) and (b) show the X-cross sections with different number of pairs (design 1-1 to 1-3) and different degree of arcs (design 2-1 to 2-3), respectively. (c) and (d) show the cross sections along $Y = 0$ with respect to (a) and (b), respectively.

B. Degree of Arc (D_a)

The design parameters are listed in design 2-1 to 2-3 of Table I, and the corresponding simulated results are shown in Figs. 4(d)–(f). The results show that, if we change the degree of arc (D_a) of a FIDT, the total amplitude fields become much more different. This shortcoming can be avoided as long as D_a is not too small [Figs. 4(e) and (f)]. Fig. 5(b) shows that, with the increasing of D_a, the beamwidth compression a ratio become larger but the amplitude remains almost constant. In Fig. 5(d), we find that the amplitude field has a peak at about 1.5 times the f_L when D_a is not too small. In contrary, when D_a is too

small, the amplitude field has no obvious peak, but a corresponding SAW beam that maintains half of its maximum until about four times the f_L.

C. Geometric Focal Length (f_L)

The design parameters are listed in design 3-1 to 3-3 of Table I, and the corresponding simulated results are shown in Figs. 4(g)–(i). As shown in Fig. 4(g), if the geometric focal length (f_L) is too small, the total amplitude field becomes unstable. With the increasing of f_L, as shown in Figs. 4(h) and (i), the total amplitude field becomes gradually identical. That is, f_L should not be too small in order to obtain stable focusing properties.
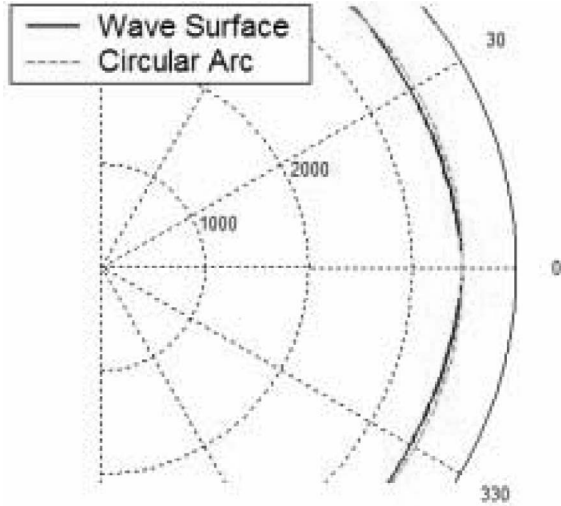
Fig. 6. Wave surface of Y-Z LiNbO$_3$.

IV. FIDTs With the Shape as the Concentric Wave Surface

A FIDT with the shape as the wave surface was first proposed by Kharusi and Farnell [11]. They reported that its focusing ability is better than that of the FIDTs with the circular-arc shape. The wave surface is the locus of points tracked by the end of the energy velocity vector $\overline{v}_e$ and is drawn from a fixed original point O as the propagation direction varies. For a plane wave, the projection of the energy velocity vector onto the propagation direction is equal to the magnitude of phase velocity vector, that is:

$$\overline{v}_e \cdot \overline{\eta} = v, \tag{6}$$

where $\overline{n}$ is the propagation direction vector and v is the magnitude of the phase velocity vector in $\overline{n}$ direction. In this paper, we adopted the effective permittivity approach to calculate the phase velocities in different propagation directions. By this approach, the ASoW theory can be extended to analyze a layered SAW device in the future [15], [16]. Based on (6), the wave surface of Y-Z LiNbO$_3$ is obtained and shown in Fig. 6. The result shows that the curvature of a circular arc is somewhat smaller than that of the wave surface.

In this section, we also use the concentric structure as the shape of the FIDT due to the same reason stated in Section III. The total amplitude field of the FIDT with the shape as the concentric wave surface was calculated by using the ASoW theory. But $\Delta(X_i')$ in (4) should be replaced with the path difference between the real aperture and the equivalent aperture of the ith finger of the FIDT. The locus of the FIDT can be determined by the polar coordinate $(\zeta_N v_e(\Phi), \Phi)$, in which Φ represents the direction of the energy velocity and $\zeta_N v_e(\Phi)$ is the corresponding radius. ζ_N is a proportional constant and is defined as:

$$\zeta_N = (f_L + Np) \frac{v_e(\Phi)}{v_e(\Phi_0)}, \tag{7}$$

where $v_e(\Phi_0)$ means the energy velocity in the main propagation direction and N is the number of fingers of the FIDT. The value of Φ depends on the desired portion of wave surface.

In the following, the design parameters in Table I also are adopted to discuss the variation of the amplitude field of FIDTs with the shape as the concentric wave surface.

A. Number of Pairs (N_p)

The design parameters are listed in design 1-1 to 1-3 of Table I, and the corresponding simulated results are shown in Figs. 7(a)–(c). These figures show that no matter how many N_p are, the total amplitude fields are quite similar and symmetric. Furthermore, the total amplitude field has a focal point, not a narrow, long, strong SAW beam. In Fig. 8(a), we see that, when adjusting N_p, the amplitude is proportional to N_p and the size of the focal area makes no obvious change. In addition, Fig. 8(c) shows that the maximum of the amplitude field is located at 0.9 times of f_L. In other words, the real focal length is somewhat shorter than the geometric focal length.

B. Degree of Arc (D_a)

The design parameters are listed in design 2-1 to 2-3 of Table I, and the corresponding simulated results are shown in Figs. 7(d)–(f). In Figs. 7(d)–(f), we observe that the total amplitude fields make significant difference when we change D_a. This shortcoming can be avoided as long as D_a is not too small [Figs. 7(e) and (f)]. As shown in Figs. 8(b) and (d), the energy of the generated SAW is highly focused on the focal area, and the real focal length appears at around 0.9 times the f_L. With the increasing of D_a, the size of the focal area become smaller. If D_a is too small, the focal area will be unobvious. That is, if we want to focus the energy of the generated SAW at a point effectively, the degree of arc should not be too small.

C. Geometric Focal Length (f_L)

The design parameters are listed in design 3-1 to 3-3 of Table I, and the corresponding simulated results are shown in Figs. 7(g)–(i). The results show that, with the increasing of f_L, the size of the focal area becomes smaller. In other words, a larger f_L lets the focal area approach to a focal point, but the size of the transducer also becomes larger.

V. Focusing Properties of GaAs Substrate

Two types of FIDTs discussed in Section III, including the shapes as a concentric circular arc and the concentric wave surface, were both on Y-Z LiNbO$_3$. In this section, we discuss the focusing properties of FIDTs on the (100)-oriented GaAs substrate.

For a FIDT with the shape as a concentric circular arc, the simulated results are shown in Fig. 9(a) and the corresponding design parameters are listed in design 1-2 of
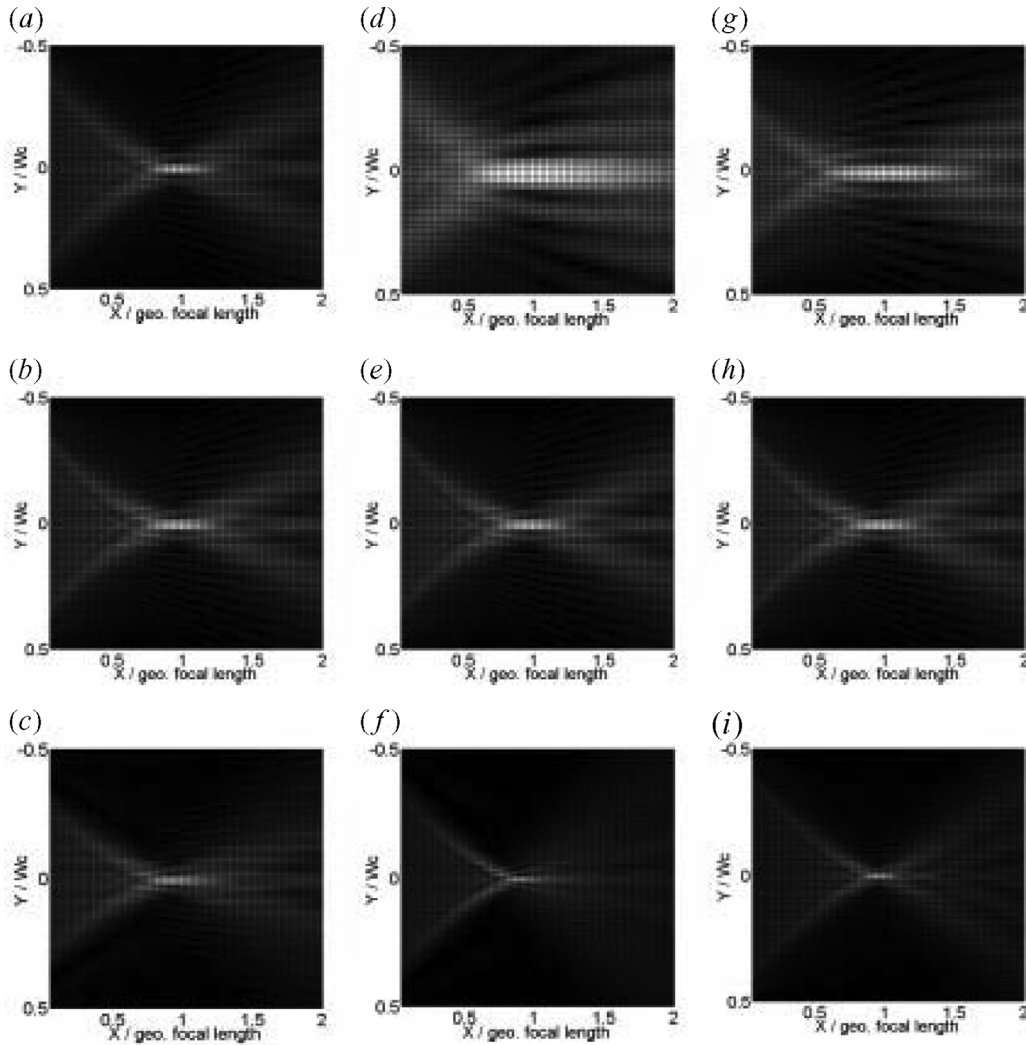
Fig. 7. Total amplitude fields of FIDTs with the shape as the concentric wave surface. (a) Design 1-1, (b) design 1-2, (c) design 1-3, (d) design 2-1, (e) design 2-2, (f) design 2-3, (g) design 3-1, (h) design 3-2, (i) design 3-3.

Table I. In Fig. 9(a), the shape of the total amplitude field is close to a focal point, not a SAW beam. In other words, a FIDT with a shape as a concentric circular arc cannot generate a SAW beam. The wave surface of GaAs and a circular arc are shown in Fig. 10. We observe that the wave surface is almost consistent with the circular arc. This is the reason why the amplitude field has a focal point, not a SAW beam. The results in Fig. 6 show that, if the curvature of a circular arc is a little lower than that of the wave surface, the amplitude field has a SAW beam. To verify this point of view, we chose a concentric elliptic arc, whose long axis is 1.8 times of the short axis, as the shape of the FIDT. The short axis of the concentric elliptic arc is along the main SAW propagation direction. The corresponding simulated results are shown in Fig. 9(b), and the design parameters are the same as that of Fig. 9(a). The results show that its amplitude field indeed has a narrow, long, strong SAW beam. In conclusion, no matter what the substrate is, we can generate a desired acoustic field that probably has a focal point or a beam, by adjusting the shape of a FIDT.

VI. DESIGN OF FIDTs

Through the above analyses, we summarized the guiderules for designing a FIDT with the desired focusing properties as follows:

A. The Focusing Property

The finger's shape of a conventional FIDT (as shown in Fig. 1) is a circular arc. This leads to a poor focusing as the number of pairs increases. In order to overcome the drawback, the FIDT's shape is suggested to be a concentric arc. As discussed in Section III, the amplitude fields of the FIDTs with different number of pairs are very stable by using the concentric arc. In addition, the results of Figs. 4(g)–(i) and Figs. 7(g)–(i) show that the geometric focal lengths should not be too small in order to acquire better focusing properties.
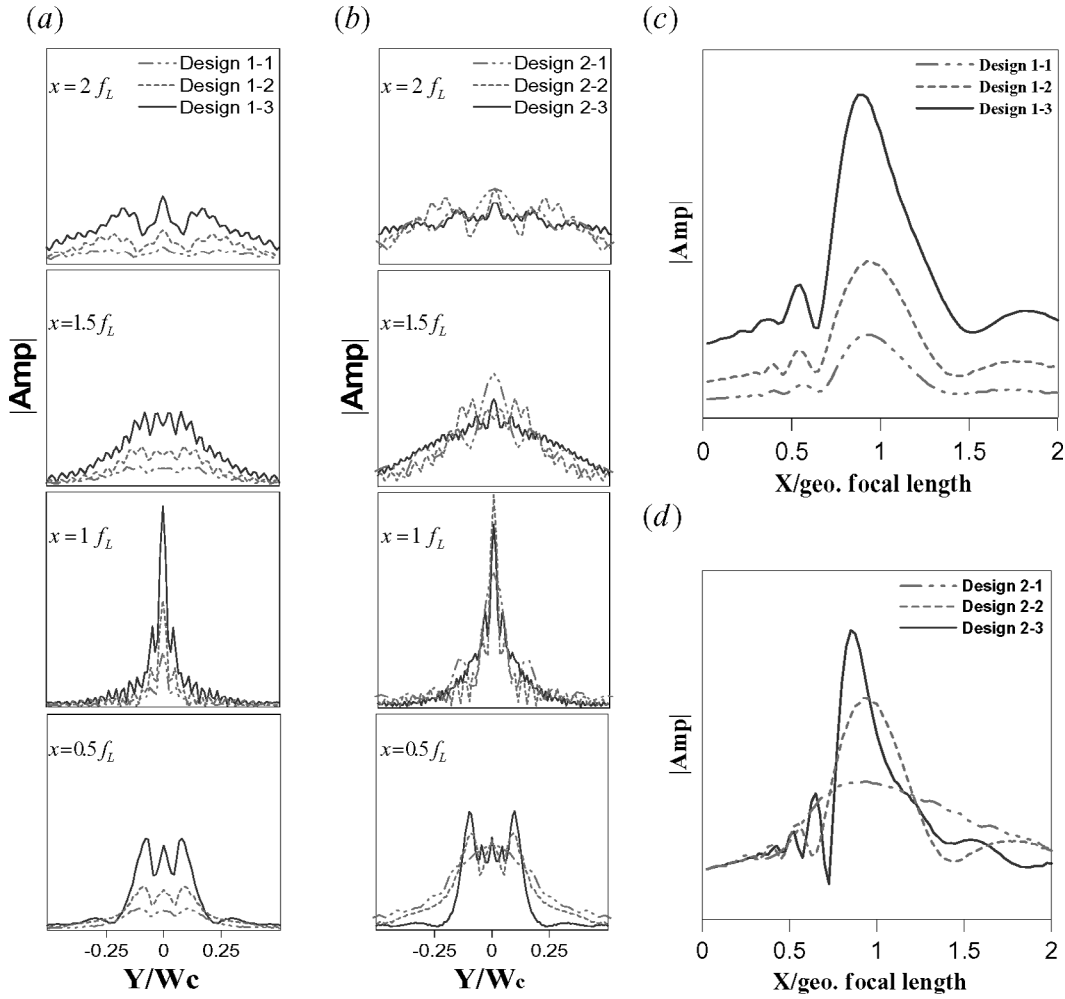
Fig. 8. Cross sections of amplitude fields of FIDTs with the shape as the concentric wave surface. (a) and (b) show the X-cross sections of amplitude fields with different number of pairs (design 1-1 through 1-3) and different degree of arcs (design 2-1 through 2-3), respectively. (c) and (d) show the cross sections along $Y = 0$ with respect to (a) and (b), respectively.

B. Intensity

As seen in Section III, the amplitude of SAW is directly proportional to the number of pairs of a FIDT. Increasing the degree of arcs of a FIDT cannot enlarge the amplitude obviously. This is because the intensity of the SAW is defined as:

$$I(X, Y) = |\psi_T(X, Y)|^2, \tag{8}$$

and the intensity of the generated SAW is proportional to the square of the number of pairs of a FIDT.

C. Beamwidth Compression Ratio

In Section III, we find that the beamwidth compression ratio depends on the degree of arc of a FIDT. The bigger the degree of arc, the larger the compression ratio. Fig. 11 shows the comparisons of beamwidth compression ratio between a FIDT and a straight IDT on Y-Z LiNbO₃. The corresponding design parameters are listed in design 1-3 of Table I. As shown in Fig. 11, the intensity and compression ratio of a FIDT are much larger than those of a straight

IDT. In addition, the intensity and compression ratio of a FIDT with the shape as the concentric wave surface are bigger than those of a FIDT with the shape as a concentric circular arc.

D. Source Type

To excite a localized spot, a FIDT with the shape as the concentric wave surface is recommended. However, to generate a narrow, long, strong line SAW source, a FIDT with the shape as a concentric circular arc is not suitable due to the anisotropy of the substrate. It is suggested to adopt a FIDT with the shape as a concentric elliptic arc whose curvature is somewhat smaller than that of wave surface.

VII. Conclusions

In this paper, we systematically studied the focusing properties of FIDTs. The ASoW theory was adopted to calculate the amplitude fields of FIDTs with a variety of geometric shapes. Because the FIDT with the shape as a concentric arc has better focusing properties, the FIDTs
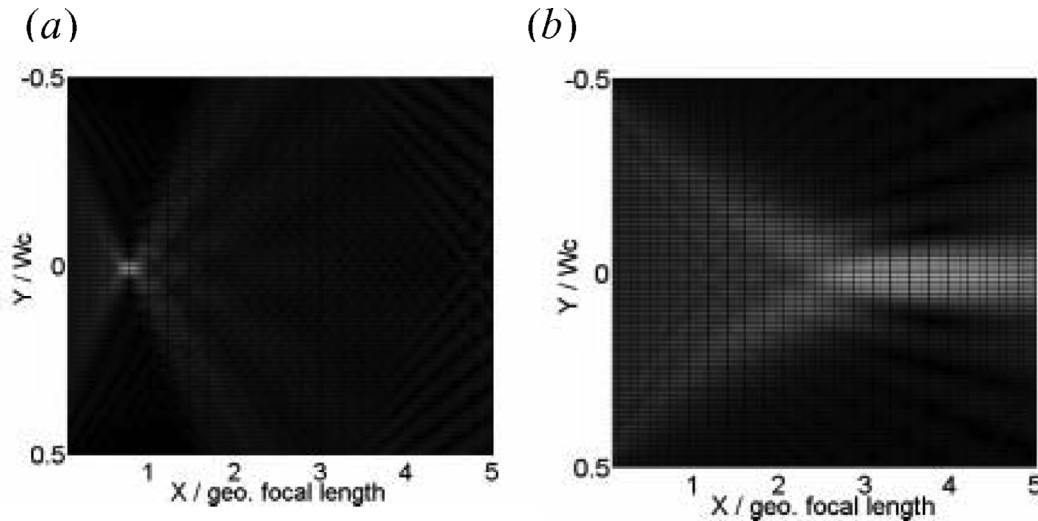
(a)

(b)

Fig. 9. Total amplitude fields of FIDTs on the (100)-oriented GaAs substrate. (a) FIDT with the shape as a concentric circular arc. (b) FIDT with the shape as a concentric elliptic arc.
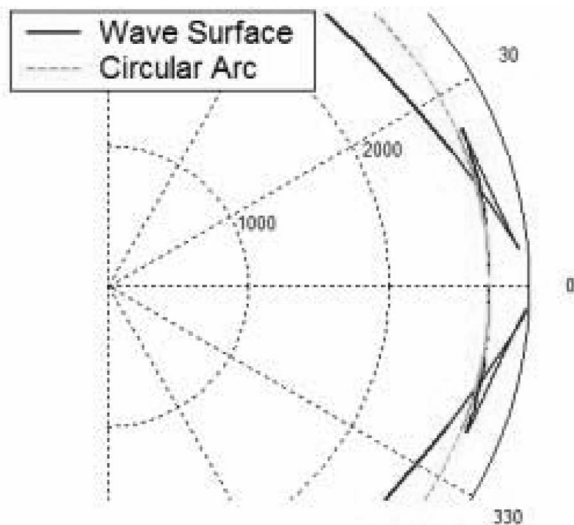

Fig. 10. Wave surface of (100)-oriented GaAs.

with the shape as a concentric circular arc and the concentric wave surface are analyzed, respectively. The results show that, for a FIDT with a concentric arc, the amplitude field is not sensitive to the number of pairs. The geometric focal length should not be too small in order to obtain a better focusing property. To excite a localized spot, a FIDT with the shape as the concentric wave surface is suggested. However, to generate a narrow, long, strong line SAW source, a FIDT with somewhat smaller curvature of the transducer than the curvature of the wave surface is needed. In addition, we suggest that a FIDT with the shape as a concentric elliptic arc is suitable for this purpose. It is worth noting that the results of this study provide an important basis for designing various FIDTs to fit the desired applications. In order to enhance the intensity of the generated amplitude fields, several design methods of conventional SAW devices, such as withdraw weighting,

single phase unidirectional transducers (SPUDT) ... etc., also can be further applied to design FIDTs.

REFERENCES

[1] J. B. Green, G. S. Kino, and B. T. Khuri-Yakub, "SAW convolvers using focusing interdigital transducers," *IEEE Trans. Sonics Ultrason.*, vol. 30, pp. 43–50, 1983.

[2] J. B. Green, G. S. Kino, and B. T. Khuri-Yakub, "Focused surface wave transducers on anisotropic substrates: A theory develop for the waveguided storage correlator," in *Proc. IEEE Ultrason. Symp.*, 1980, pp. 69–73.

[3] T. J. Marynowski, "Focusing transducers for SAW beamwidth compression on YZ lithium niobate," in *Proc. IEEE Ultrason. Symp.*, 1982, pp. 160–165.

[4] Y. Nakagawa, "A new SAW convolver using multi-channel waveguide," in *Proc. IEEE Ultrason. Symp.*, 1991, pp. 255–258.

[5] J. Z. Wilcox and R. E. Brooks, "Time-Fourier transform by a focusing array of phased surface acoustic wave transducers," *J. Appl. Phys.*, vol. 58, no. 3, pp. 1148–1159, 1985.

[6] R. E. Brooks and J. Z. Wilcox, "SAW RF spectrum analyzer/channelizer using a focusing, phased array transducer," in *Proc. IEEE Ultrason. Symp.*, 1985, pp. 91–95.

[7] A. Kar-Roy and C. S. Tsai, "Focused SAW induced sidelobe suppression of integrated acousto-optic tunable wavelength filters," in *Proc. IEEE Ultrason. Symp.*, 1992, pp. 169–172.

[8] A. Kar-Roy and C. S. Tsai, "Low-sidelobe weighted-coupled integrated acoustooptic tunable filter using focused surface acoustic wave," *IEEE Photonics Technol. Lett.*, vol. 4, no. 10, pp. 1132–1135, 1992.

[9] M. M. de Lima, R. Hey, Jr., J. A. H. Stotz, and P. V. Santos, "Acoustic manipulation of electron-hole pairs in GaAs at room temperature," *Appl. Phys. Lett.*, vol. 84, pp. 2569–2571, 2004.

[10] T.-T. Wu, L.-C. Wu, and Z.-G. Huang, "Frequency band-gap measurement of two-dimensional air/silicon phononic crystals using layered slanted finger interdigital transducers," *J. Appl. Phys.*, vol. 97, article No. 094916, 2005.

[11] M. S. Kharusi and G. W. Farnell, "On diffraction and focusing in anisotropic crystals," *Proc. IEEE*, vol. 60, no. 8, pp. 945–956, 1972.

[12] S. R. Fang and S. Y. Zhang, "SAW focusing by circular-arc interdigital transducers on YZ-LiNbO₃," *IEEE Trans. Ultrason., Ferroelect., Freq. Contr.*, vol. 36, no. 2, pp. 178–184, 1989.

[13] M. M. de Lima, R. Hey, Jr., W. Seidel, and P. V. Santos, "Focusing of surface-acoustic-wave fields on (100) GaAs surface," *J. Appl. Phys.*, vol. 94, no. 12, pp. 7848–7855, 2003.
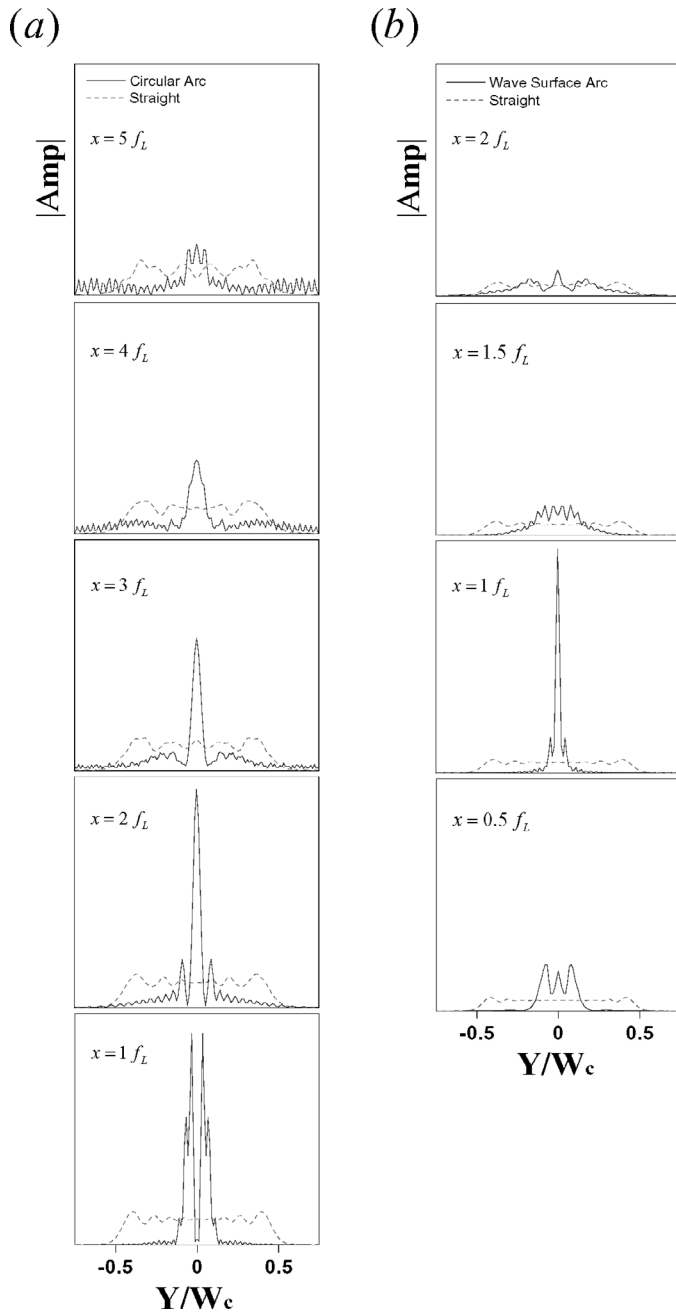
(a) (b)

Fig. 11. Beamwidth compression ratios of FIDTs on Y-Z LiNbO$_3$. (a) Concentric circular arc versus straight. (b) Concentric wave surface versus straight.

[14] D. P. Morgan, *Surface-Wave Devices for Signal Processing*. New York: Elsevier, 1985, pp. 129–155.

[15] T. T. Wu and Y. Y. Chen, "Exact analysis of dispersive SAW devices on ZnO/diamond/Si layered structures," *IEEE Trans. Ultrason., Ferroelect., Freq. Contr.*, vol. 49, pp. 142–149, Jan. 2002.

[16] Y. Y. Chen, T. T. Wu, and C. T. Chou, "Analysis of the frequency response of a dispersive IDT/ZnO/sapphire SAW filter using effectivity and coupling of modes model," *J. Physics D: Appl. Phys.*, vol. 37, pp. 120–127, 2004.

Tsung-Tsong Wu received his B.S. degree from National Taiwan University in 1977, and M.S. and Ph.D. degrees in theoretical and applied mechanics from Cornell University in 1983 and 1987, respectively. He joined the faculty of National Taiwan University in 1987, and currently is professor of the Institute of Applied Mechanics.

His research interests are in high frequency ultrasonics and related precision measurement techniques. Particular interests include advanced SAW devices, phononic crystals, and nondestructive evaluation of materials.

He-Tai Tang received his B.S. degree from National Taiwan Ocean University in 2002 and M.S. degrees from the Institute of Applied Mechanics, National Taiwan University in 2004. He currently is on active military duty. His research interests are theoretical analysis and experiments of SAW devices.

Yung-Yu Chen received his B.S. degree from National Chen-Kung University in 1995 and Ph.D. degrees from the Institute of Applied Mechanics, National Taiwan University in 2002. He is currently post doctor of the Institute of Applied Mechanics, National Taiwan University. His research interests are surface waves in layered anisotropic and/or piezoelectric materials, SAW devices and related sensors.

Pei-Ling Liu was born in Taiwan in 1956. She received the B.E. and M.S. degrees in civil engineering from National Taiwan University in 1979 and 1981, respectively, and the Ph.D. degree in civil engineering from the University of California, Berkeley in 1989. She joined the faculty of the Institute of Applied Mechanics, National Taiwan University in 1989. She is currently the director of the Institute. Her major research fields are nondestructive evaluation of structures, structural reliability, and elastic waves. She is a member of the American Society of Civil Engineers.